Design, Construction and Performance Evaluation of a Cold Gas Thruster Test Stand

Alireza Alikhani[1*] and Mohammad Reza Salimi[2]

Aerospace Research Institute, Ministry of Science, Research and Technology, Tehran, Iran

*Corresponding Author's E-mail: aalikhani@ari.ac.ir

Abstract

The cold gas thruster is one of the significant components of a satellite and its application possesses a marked impact on the entire system performance. The nonlinear function and order of magnitude, lead to increasing the importance of thruster function. Therefore, pre-mission performance assessment has a considerable effect on the risk reduction of space missions. In this article, an uncomplicated and efficient pendulum scheme for development and implementation of a Thruster Test Stand (TTS), to measure the thrust produced at the end of the nozzle is proposed. The TTS is capable of measuring thrust levels in the range of 0.1Newtons to 3N with operating frequencies up to 50 Hz, which is used by various satellite ranges. The experimental results demonstrate that although the designed device is less sophisticated than other test devices, it is capable of measuring the produced thrust very precisely and with less than 15mN.

Keywords: Cold gas thruster, Test stand, Nozzle, Satellite mission, Measurement

Nomenclature

TFMS	Thrust Force Measurement System
TTS	Thruster Test Stand
CSS	Control and Software System
γ	thermal capacity ratio

Introduction

Propulsion system plays a significant role in the satellite operation for a wide range of missions, including orbit transformation, attitude maneuvers, orbital station keeping, etc. The cold gas thrusters are one of the main types of propulsion systems widely used in the satellite or spacecraft to produce the required torque or force. The undeniable fact that the performance of each component of the cold gas propulsion will have a significant impact on the overall system efficiency and in some cases could lead to a mission failure. In order to accurately simulate and implement the satellite attitude control system, determining the exact amount of applied trust as well as development of a numerical model of the nozzle flow are essential. In order to evaluate the propulsion system performance, the precise measurement process should be developed. High level of rocket thrust production and their lower sensitivity, make it possible to employ a load cell to measure their forces. On the other hand, low thrust level systems, such as cold gas, necessitate the use of much more sensitive measurement techniques. Diverse approaches have been proposed for determining the performances of cold gas thruster that can be classified into three main categories as hanging pendulum, inverted pendulum, and torsional pendulum design [1, 2].

The hanging pendulum mechanism is a method that has been employed generally in the literature. This mechanism is extremely stable by eliminating external forces that may cause a crucial disturbance in the measurement process. Additionally, sensitivity can be regained by increasing the length of the pendulum arm or by adding a counterweight to adjust the mass center along the cable to remove the gravity torque [3-6]. Moeller et al [7] developed a complex mechanism based on the hanging pendulum that measures the electric propulsion thrust operating in the vertical direction. An adjustable mechanical linkage system is employed to convert the thruster-induced deflection of a primary part into deflections of a secondary beam that measurement device is located on it. In [8], a test stand was

---

1. Associate Professor
2. Assistant Professor

developed using a quasi-one-dimensional theory based on the ballistic-pendulum principle. This system is capable of measuring small cold-gas nozzles ranging around 0.1 N and a specific impulse of the order of 10 s.

The inverted pendulum configuration is unstable but possesses a wide range of sensitivity depending on the stiffness of the flexures and load spring. The inverted pendulum has been employed to identify the performance of the electronic propulsion devices, including resist jets, electro-thermal arc jets, MPD thrusters, Hall thrusters, and ion engines [9-11]. Kunning et al. developed a system to measure thrust over a range of 1 mN to 5 N. The design uses a conventional inverted pendulum and in order to improve sensitivity, a null-type feature is the added to the structure to eliminate thrust alignment error due to deflection of thrust. Also, mechanical oscillations are actively damped during the test process by an electromagnetic damper [12]. The disadvantage of the inverted pendulum is regarding the stability and sensitivity factors, which are vital factors of this mechanism, which may be affected by external factors such as temperature and external vibrations.

The torsional configuration due to the independence of restoring force and thruster provides high sensitivity estimation. This advantage is caused by the parallel axis of rotation and gravity vector [13-15] (unlike the hanging or inverted pendulum). Koizumi et al. [16] fabricated a torsional test stand for pulsed plasma micro-Newton level thrusters, and developed a specific method for filtering the disturbance effect such as mechanical vibrations on the system In [17, 20] a torsional pendulum with a low natural frequency was developed and the magnitude of the oscillation resulting from the thrust was used to measure the impulse delivered. The designed stand cannot damp vibration actively, and operates with less time between impulses than the oscillations take to decay. Lugini [21] developed a test stand for cold gas thrusters based on the ballistic-pendulum principle. This stand is equipped with a fin, immersed in water, to provide torsional and lateral oscillation damping. A laser sensor measures the displacement of pendulum.

The objective of this research is to propose a new scheme using a pendulum approach to measure the thruster force ranging 0.1-3 N. The calibration process to enhance the system accuracy is taken into account and a diverse mechanism to increase the system accuracy is investigated. The most important advantage of the proposed system is that using uncomplicated mechanism, it provides high accuracy and efficiency. The experimental results demonstrate that although the designed device is less sophisticated than other test devices, it is capable of measuring the produced thrust very precisely and with less than 15mN. The paper is organized as follows; in section 2, the experimental setup with constitute units is proposed. The equation of nozzle design to determine geometric parameters is presented in section 3. In the following, the numerical simulation of

the designed nozzle is investigated in the section 4. The experimental results to compare numerical design to ensure the TTS performance are demonstrated in section 5. Finally, conclusions are drawn in section 6.

Experimental Setup

The Thruster Test Stand (TTS) is carried out to measure the produced force by a cold gas thruster using ballistic-pendulum approach. This mechanism measures the impulse transferred to the thrust plate by a load cell directly. The TTS design, considered all the frictional condition at the interface between diverse components to enhance the accuracy of results. The schematic of TTS design can be observed in Fig 1.
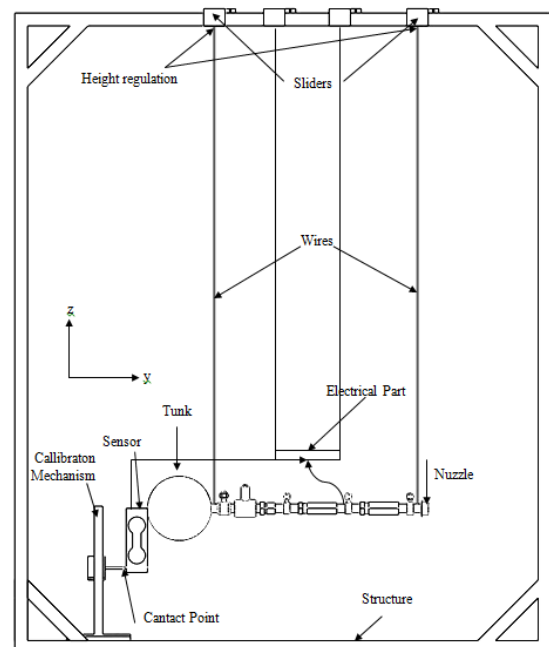

Fig. 1: Schematic representation of the TTS system

As can be noticed, The TTS contains different components which connect together in order to accomplish the purpose of the system. The TTS includes four main sections: structure, propulsion system, electrical components, and calibration mechanism, which are explained in detail in the following.

Structure

The structure is a rigid platform including some special portions to hang the measurement pendulum system with the least vibration and external forces. This rigid structure contains some beams and wires to suspend the electrical and propulsion parts. The hanging system is suspended from a pivot so that it can swing freely. It is worth considering that, system balancing to eliminate the impact of the gravity force on the system performance is significantly vital. Hence, the elaborate approach using regulation of

wire height is employed to balance the hanging part. Furthermore, two sliding mass was designed to hang the cables vertically without any deviation. An electro-optic laser has also been employed to ensure the absence of deviation angle. The horizontal alignment screws are used to align the structure perfectly.
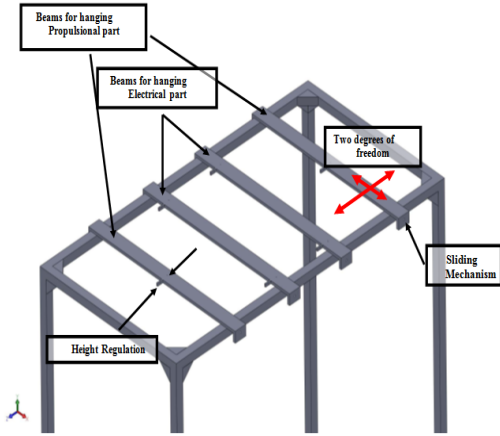

Fig. 2. The mechanism for hanging system

The precision measurement which can be affected by vibration is another factor that has been taken into consideration during the design process since it may lead to the reduce measurements accuracy. Accordingly, the structure and its mass properties are designed in such a way to eliminate this disturbance effect. The TTS structural outline is illustrated in the figure 3.
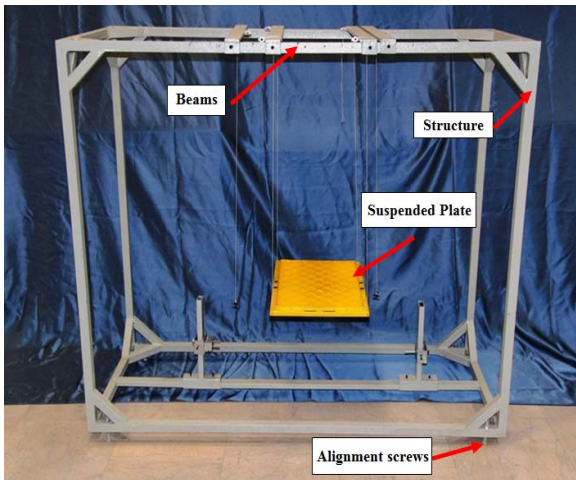

Fig. 3: The TTS structural outline

The structures provide suitable conditions for the installation of other electrical and propulsion components in order to function properly. Also, the material used to fabricate this construction is aluminum alloy which is durable, lightweight, and can provide sufficient stability.

One of the critical parts of this design process concerns preparing a horizontal plate for the propulsion system. This issue during the structure design should be considered since gravitational force should be removed in this system. For this reason, two distinct strategies are adopted for plate balancing. Firstly, four alignment screws to balance the structure are considered which can be adjusted manually. A digital level tool is employed to adjust the screws in a high precision to confirm horizontality.
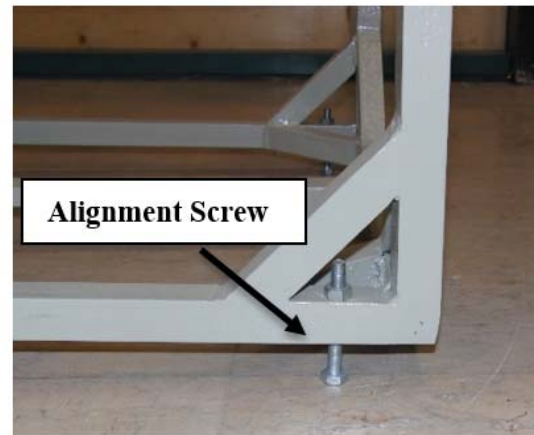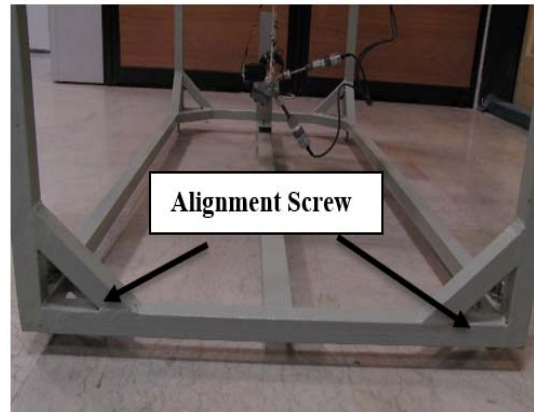

Fig 4: The alignment screws to prepare horizontal plate

Secondly, in order to set the propulsion plate parallel to the surface, the height of the wire can be changed by two screws named height regulation. Despite this mechanism, two sliding booms are designed to change the position of the suspended system. Using these sliding masses plays a remarkable role to adjust the distance between the electrical plate and the propulsion system. Apart from the high precision digital level tool, an electro-optic laser is employed to regulate wires and sliding masses.
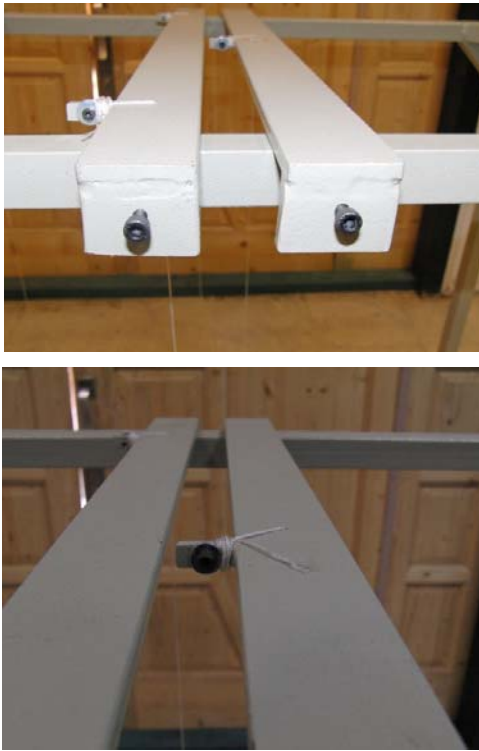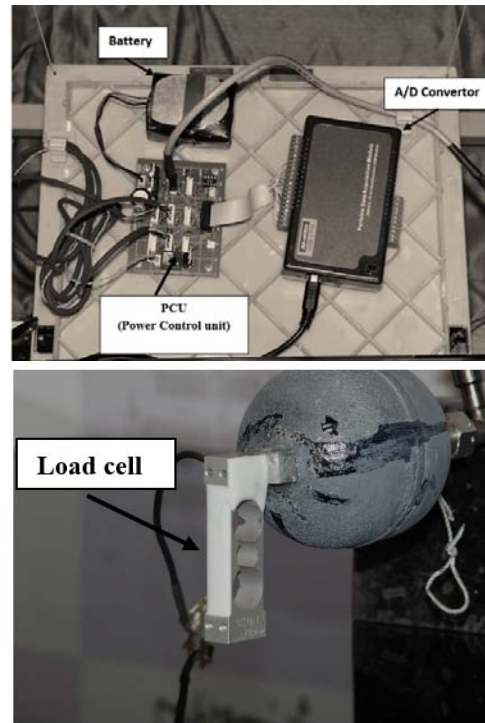
Fig. 5: Suspending equipment

Fig. 6: The Control Unit

Control and Software System (CSS)

A complete set of electrical instruments are arranged in order to control the propulsion system and to monitor the thrust force data. The sensor used to measure the thrust is a load cell with a maximum load of 300 grams. This sensor with accuracy of about 0.5mN has an adequate range to measure the thrust force. A power control unit to supply voltage of 5 V, 9 V and 18 V for the pressure sensor, load-cell, and opening the solenoid valve is considered. Furthermore, for acquisition of data, a 16 bit analog to digital converter with high sampling rate is used to transfer data from the sensor to a computer. The overview of the control unit is represented in the Fig. 6.

In order to analyze data from the propulsion system, special software named Thrust Force Measurement System (TFMS) has been designed. This software is enabled to display the force produced by thruster during its application online. The overview of the TFMS software is represented as Fig. 7.

As can be observed, two individual graphs are considered for online display of collected data by sensors. In the first graph, the thrust and anti-trust measured by load cells are displayed. Also, the pressure in different parts of the propulsion system such as Tank and Nozzle are exhibited in the next graph. It's worth noting that, in the general part of this software the sample rate of data, as well as a low pass filter, are considered that users can select these features based on their requirements.
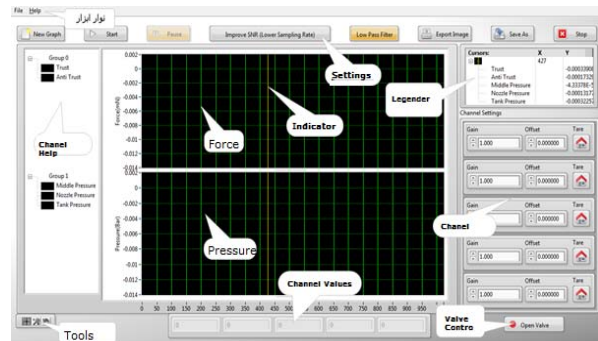

Fig. 7: The overview of TFMS software

Propulsion System (PS)

The propulsion unit is the main section of TTS that includes a diverse component to produce desire force. The propellant can be at a maximum pressure of 150 bar stored in a high-pressure composite tank. A relief valve is connected to the tank directly to limit the maximum pressure in the circuit. Two-stage cylinder regulators reduce the high pressure from approximately 150 to 20 bar which is finally connected to the nozzle. Three analogue sensors to measure pressure are assembled along the pressure line. These sensors are arranged in three critical points as after the tank, after the first regulator, and back of the nozzle. The solenoid valve occurs between fuel tank and regulators, and operates by an electrical signal from the controller.

Calibration Process

This section describes the TTS calibration procedure that plays an important role to reach precise results. In order to obtain proper measurements, the system should start from a rest condition. Hence, there must be no external vibration around the test stand. Furthermore, since the propulsion system is suspended by wire, the absence of any oscillation is necessary for an appropriate diagnosis. This process consists of two steps that should be implemented appropriately. Firstly, the bias force level of the load cell should be determined. This phase is inevitable in determining the pure generate force by the nozzle. Before carrying out the nozzle test, the load cell should be in contact with a small beam to calculate the initial force on it. This process can be observed in the Fig. 9.

This amount should be subtracted from the nozzle trust measurement. As can be shown, the small beams are contacted to load cell to apply force on it. The next calibration phase is concerning disturbance force on the system such as balancing. This step is required to identify the disturbance force on the load cell that may cause deviations and errors in calculations. Using two sensors on both sides of the mechanism makes it possible to ensure the effects of these disturbances such as gravitational force on the system performance. In this strategy, by applying specific force along the horizontal vector, two load cells are supposed to measure same forces. The measurement variation between two load cells should be considered in calculating the Nozzle force. This approach is demonstrated in Fig. 10.
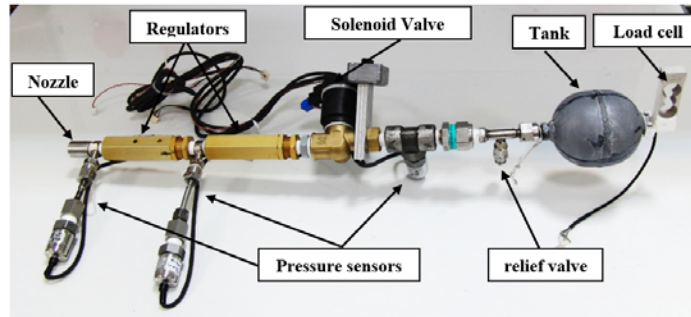

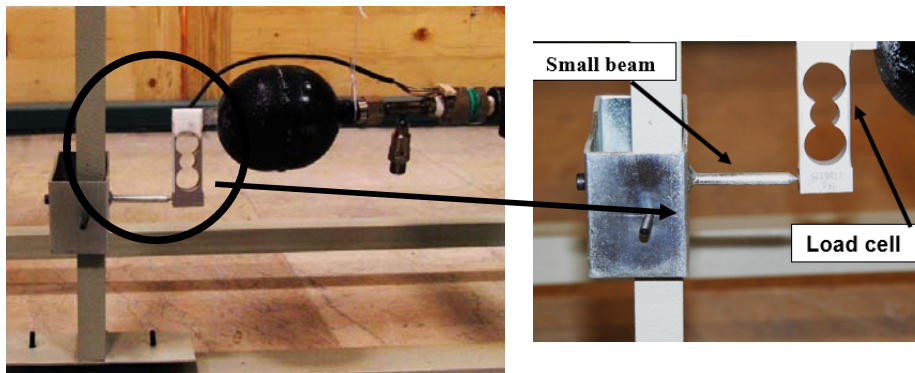
Fig. 8: The Propulsion System
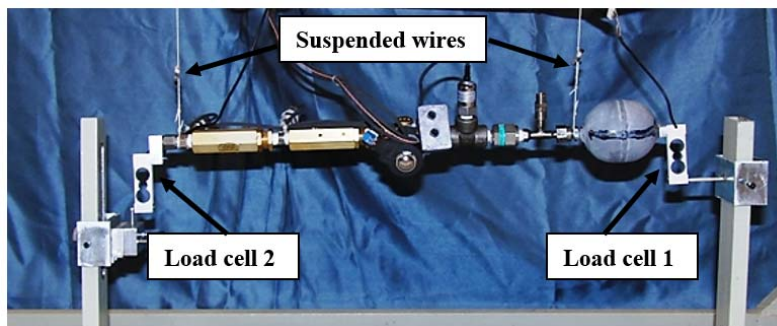

Fig. 9: Load cell calibration process

Fig. 10: Gravitational force measurement

Thruster Test Stand (TTS)

As stated, the thruster test stand including various parts and the overall view of this system is shown in Fig. 10. Since this system is a high accuracy test set up, the development process including design, fabrication, integration and implementation were performed elaborately.
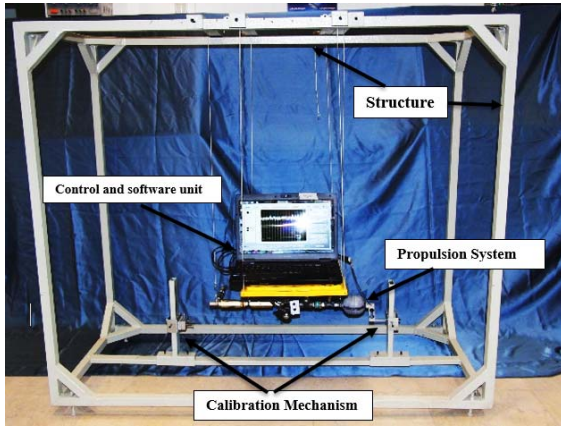

Fig. 11: Thruster Test Stand

It should be noted that, the PS and CSS subsystems are mounted on different plates suspended individually by wires. These two subsystems are connected together with cables of sensors and solenoid valve that have very low impact on the system measurement. The system can be started by user command and all the data between user and TSS are transferred wirelessly.
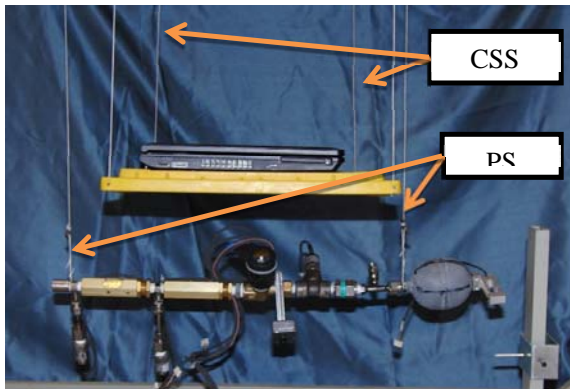

Fig. 12: The wires of CSS and PS system

Geometric Design of Nozzle

A nozzle is a tube with variable cross-sectional area (often axisymmetric) aiming at increasing the speed of a stream, controlling the direction as well as the shape of exiting flow. The basis of nozzle application is force generating associated with the change in the flow momentum. The flow in a nozzle is very rapid, and friction factor is negligible. The isentropic model all along the nozzle can be considered to design the nozzle, since the flow is nearly one-dimensional with a desirable pressure gradient except for shock waves condition and also the nozzles are relatively short.

The quasi one-dimensional theory is used to design the nozzle geometry, as explained in the following [18, 19]. The basic hypotheses are defined as:

1. The fluid is a perfect gas,
2. No phase change occurred inside the nozzle,
3. The geometry of the nozzle and the flow is symmetric,
4. There is no shock wave and discontinuity in the nozzle flow,
5. Upper throat conditions are the same conditions after tap valve.

In the design process, there are limitations applied to other parts of the propulsion system, but affect the design of the nozzle. In the following, two important constraints of design and manufacturing are mentioned:

1. The nozzle throat diameter cannot be less than (0.5 mm) due to construction constraints,

2. The outlet area of the regulator must be at least two to three times the area of the nozzle throat. Hence, in order to prevent strangulation of the flow, and since the outlet diameter of regulator is considered 1mm, the diameter of the throttling nozzle should not be more than 0.71mm.

The equations related to the geometry design of the nozzle are explained in the following.

By knowing the ratio between the total pressure and the pressure at exit plane, the Mach number at the exit area is obtained.

$$\frac{P_0}{P_e} = \left[1 + \frac{y-1}{2}M_e^2\right]^{y/1-y}$$

$$M_e = \sqrt{\frac{2}{y-1}\left(\left(\frac{P_0}{P_e}\right)^{y-1/y} - 1\right)} \qquad (1)$$

Where γ is the thermal capacity ratio as $y = \frac{C_p}{C_v}$, P_0 the backpressure of the nozzle, and M_e is the exit Mach number.

The temperature at the exit section is written as:

$$\frac{T_0}{T_e} = \left[1 + \frac{y-1}{2}M_e^2\right] \rightarrow T_e = T_0\left(1 + \frac{y-1}{2}M_e^2\right)^{-1} \qquad (2)$$

Where T_0 and T_e are the nozzle chamber temperature and the exit stream temperature, respectively.

The sonic velocity in the gas is:

$$a_e = \sqrt{\gamma R T_e} \qquad (3)$$

Where γ is the thermal capacity ratio as $y = \dfrac{C_p}{C_v}$, R is

the gas constant, $R = \dfrac{R_u}{M}$, and with Ru=8.314 and M being the molar mass, the exit velocity is determined as:

$$V_e = M_e a_e \tag{4}$$

Finally, the thrust can be calculated by the following equation:

$$T = \dot{m}V_e + P_e A_e \tag{5}$$

It is appropriate to vary the expansion ratio, solve for each subsequent Mach number, and find the pressure ratio to solve (7):

$$\varepsilon = \frac{1}{M_e}\left[\frac{2}{\gamma+1}\left(1 + \frac{\gamma-1}{2}M_e^2\right)\right]^{(\gamma+1)/2(\gamma-1)}$$
$$A_e = \varepsilon A_{th} \tag{6}$$

The specific impulse that is one of the main parameters of a nozzle is determined as:

$$I_{SP} = \frac{T}{g\dot{m}} \tag{7}$$

The design specification of propulsion system based on the construction limitation and design equation can be observed in the table 1:

Table 1: The propulsion system characteristics parameters

Parameter	Value
Tank pressure	$P_{Tank} = 120 (atm)$
Specific Impulse	$I_{SP} = 71.1$
Condition downstream of pressure regulator	$P_C = 15(bar),\ T_C = 272(K),\ \rho_{Ch} = 18.8(kg/m^3)$
throat diameter	$D_t = 0.71(mm)$
Area expansion ratio	$\varepsilon = 17$
Nozzle convergence section half-angle	$\beta = 30$
Nozzle divergence section half-angle	$\alpha = 11^0$
Thrust	$T = 0.6511(1atm)$ $T = 1.04(Vacuum)$
Mass Flow	$\dot{m} = 0.0015(kg/s)$

Numerical Simulation

In order to validate the designed nozzle profile, flow inside nozzle is simulated numerically using FLUENT software. In this regard, flow fields in both atmospheric and vacuum conditions are simulated, and the produced thrust and the specific impulse are computed.

To this end, two -dimensional axi-symmetric simulations are performed and the resulting Mach number contours along with the flow streamlines in vacuum and atmospheric conditions are depicted in Fig. 13. As expected, flow is fully expanded in vacuum condition (Fig. 13b) and a much disc is appeared in the nozzle divergence section to adapt pack pressure in atmospheric case (Fig. 13a). As shown in Fig. 13a, the shock boundary layer interaction in atmospheric case created a massive flow separation at the nozzle exit section. This flow separation confined the high velocity jet to the center of the nozzle and reduced the thrust level in atmospheric case.

Additionally, Mach number was reduced in exit due to the shock structures, and both exit velocity and ISP in atmospheric condition decreased. It is evident from Fig. 13a that the oblique shock after collision with the central Mach disc was reflected as a secondary oblique shock. The reflected shock interacts with the surrounding constant pressure boundary and forms a series of subsequent expansions and shock waves. These wave structures change the exit jet width accordingly. To verify the reported results in Table 1 (thrust and mass flow rates), these values are computed again based on axi-symmetrical numerical simulations and are listed in Table 2. Comparing Table 1 and 2, shows a very good agreement between zero-dimensional and two-dimensional results.

Table 2: Computed mass flow rate, thrust, and Isp from numerical simulations

| Thrust(N)	$T = 0.631(1atm)$
	$T = 0.934(Vacuum)$
Mass Flow (kg/s)	$\dot{m} = 0.001457$
Isp	$I_{sp} = 65.4$
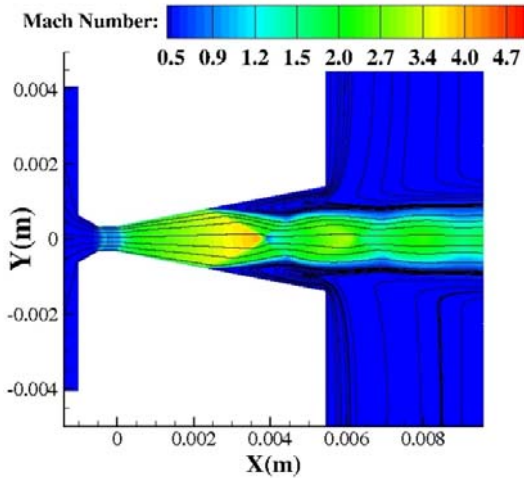
a) atmospheric condition
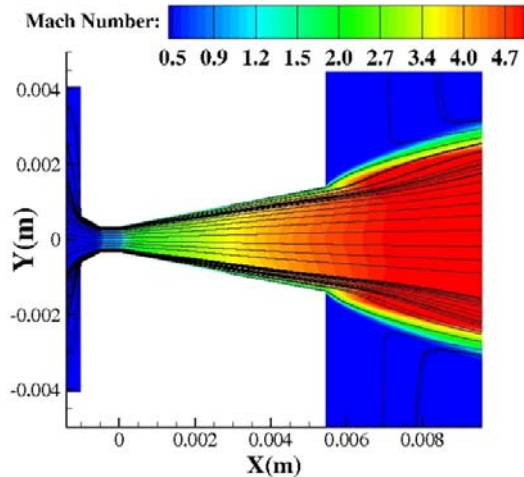
b) atmospheric condition

Fig. 13: The flow speed contours in an atmospheric condition.

After construction of designed nozzle, as indicated in Fig. 14, a small defect could be seen in nozzle throat area, which is formed due to the fabrication limitations. To examine the impact of this defect on nozzle performance, a CMM graph of nozzle's internal geometry was provided. The CMM graph was then used to simulate the flow field in three dimensions. The resulting three-dimensional iso-surfaces of velocity magnitude are shown in Fig. 15. As, indicated in this figure, defects do not affect the flow field considerably and no qualitative deviation can be seen in exit jet.
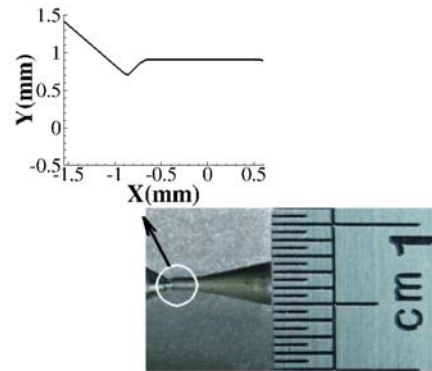

Fig. 14: Nozzle cross section image and its CMM profile

The effect of vector deviation can markedly impact on the thruster application. This issue is important in employing actuators since it may cause tremendous disturbance impact on the dynamic stability. To this end, a quantitative measurement of thrust vector deviation is essential to ensure the fabrication accuracy. According to the three dimensional simulations, the measured deviations of the thrust vector in the vacuum and atmospheric conditions are as 0.31 deg and 0.01 deg, respectively. It is clear that the vector deviation in both vacuum and atmospheric states is very low and can be neglected.

Finally, to ensure that defects in nozzle throat section do not affect the nozzle characteristic properties, mass flow rate, thrust magnitude and deviation in vacuum and atmospheric conditions are listed in Table 3. Comparing the results in Table 3, with those of Tables 1 and 2 indicates the validity of design and fabrication methods. The small difference in mass flow rate indicates that, the nozzle throat area was not affected by defects considerably.

In the next section, it will be shown that, there is a close agreement between above mentioned numerical simulations and experimental measurements.
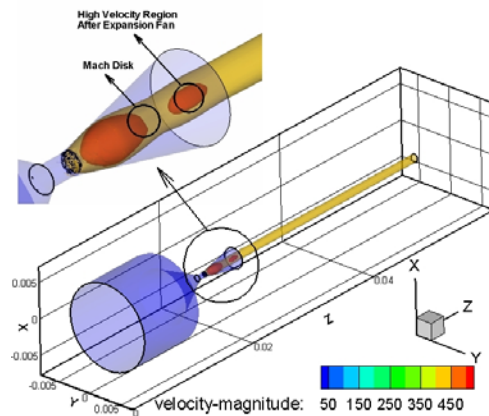
**Fig. 15**: The flow vector deviation

Table 3: Three dimensional numerical simulation results

| Parameter va	lue	
Backpressure	1 atm	vacuum
Mass Flow (kg/s)	0.00142	0.00142
Thrust(N)	0.628	0.93
X_Deviation (deg)	0.31	0.01
Y_Deviation (deg)	0.101	0.01

Experimental Results

The experimental results of the designed nozzle are discussed in this section. It is worth nothing that since we cannot provide a particular component for vacuum test as vacuum chamber, the experimental test was just applied in the atmospheric condition. The most important parameter of the thruster is the produced force. Therefore, this parameter is measured by means of thruster test stand (TTS). The detailed design of the TTS is explained in the section 2. The nozzle was fabricated according to the design specifications in the previous section. The overview of the constructed nozzle is exhibited in Fig.16.
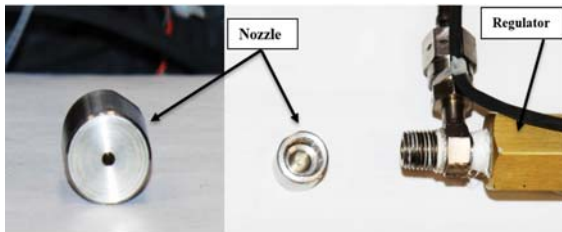

Fig. 16: The overview of the constructed nozzle

This fabricated nozzle is assembled to the end of the fuel line after a regulator. The main task of this regulator is to provide the pressure of the nozzle in the constant value (P=15bar). The measurement process starts with the valve opening. The pressure changes along the line from the tank to the nozzle during the experimental test are represented in Fig.17.
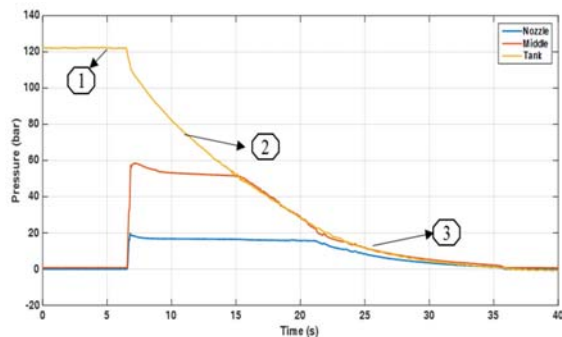
Figure 17: The pressure changes along the line

The process can be categorized into three phases that each of them are illustrated in the figure. In the first phase, it is evident that the initial pressure in tank is 120 bar and this value remains constant until the solenoid valve works. After opening the valve (phase 2), the first regulator and the nozzle pressure climb to 55 and 15 bar, respectively. Also, the tank saw a gradual pressure decline due to the fuel consumption. This condition continues until the tank pressure reaches below 55 bar and at this time the first regulator pressure begins to decrease steadily. In the following (phase3), by decreasing the first regulator pressure to approximately 15 bar, the nozzle pressure decreases from 15 bar to zero in about 20 sec. It is clear that the force produced with the nozzle has direct relation to fuel pressure that it uses. The thruster force during the experimental test is shown in the Fig. 18.
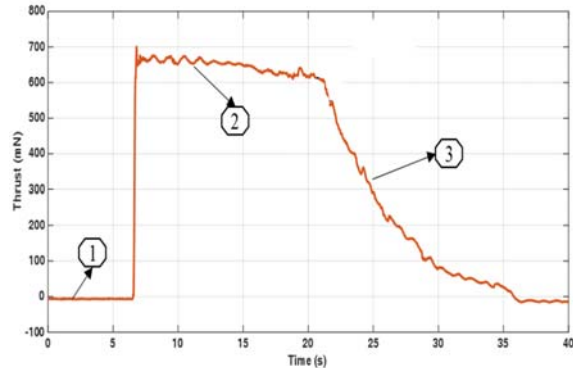
Fig. 18: The measurement of force generated by nozzle

As can be observed in the first phase, the nozzle does not produce any force due to absence of fuel pressure. In phase 2, after opening the valve, the generated force reaches to approximately 650 mN and this value is significantly depended on the backpressure. Since system does not provide constant pressure, the force generated experiences numerous oscillations during this test. By reaching the backpressure under 15 bar (phase 3), while the pressure decreases, the production force also declines. These measures continue until the tank fuel is consumed completely.

The comparisons between analytical, numerical, and experimental results are represented in Table 4.

Table 4: The comparison between analytical, numerical, and experimental results

Measurement	Trust value(mN)	
	1 atm	vacuum
Analytical	0.6511	1.04
Numerical(3D)	0.628	0.93
Numerical(2D)	0.631	0.934
Experimental	0.65	Future study

It is evident that the experimental results are close to other measurements and the accuracy of the TTS data is

below 15 mN and demonstrates the capability of this system to measure the thrust force. The differences between results may relate to some reasons as load cell accuracy, regulator performance, and environment disturbances. As indicated in Table 4, the vacuum results will be determined in the future study.

Conflict of Interest

There is no conflict of interest by the authors.

Conclusion

In this paper, a Thruster Test Stand (TTS) was proposed for accurate measurement of a nozzle thrust. The test setup includes different subsystems including structure, propulsion, and computer software that were presented clearly. The TTS approach to measure the thrust is pendulum-based and a load cell measures the produced force. The equations to design a desired nozzle were derived and nozzle's geometrical specifications were determined. The designed nozzle was fabricated and assembled on the Thruster Test Stand. The comparison between analytical, numerical, and experimental results demonstrated that the accuracy of the TTS data is below 15 mN and this system is capable to measure the force generated by the nozzle between 0.1-3 Newton.

References

[1] W. Storck, O. Billett, M. Jambusaria, A. Sadhwani, P. Jammes and J. Cutler, "A survey of micropropulsion for small satellites", Small Satellite Conference, 2006.

[2] N. Henry Gary, W. Humble Ronald, J. Larson Wiley, *Space Propulsion Analysis and Design*, Dept. of Defense, United States. National Aeronautics and Space Administration, 1995.

[3] J. Pollard, K. Diamant, M. Crofton, M. Patterson, G. Soulas, "Spatially-resolved beam current and charge-state distributions for the next ion engine," *46th AIAA/ASME/SAE/ASEE Joint Propulsion Conference & Exhibit,* p. 6779, 2010.

[4] F. Paganucci, P. Rossetti, M. Andrenucci, V.B. Tikhonov, V. A. Obukhov, "Performance of an applied field MPD thruster with a pre-ionization chamber," *In33rd Plasmadynamics and Lasers Conference,* p. 2103, 2002.

[5] A. Sasoh and Y. Arakawa, "A high-resolution thrust stand for ground tests of low-thrust space propulsion devices," *Review of Scientific instruments.* Vol. 64, no. 3, pp. 719-23, 1993.

[6] H. Sheikh et al, "Design of Test Bench for Measurement of Thrust and Impulse bits of MEMS-based Micro thrusters", *Journal of young investigators*, vol. 35, 2018.

[7] T. Moeller and K.A. Polzin, "Thrust stand for vertically oriented electric propulsion performance evaluation," *Review of Scientific Instruments*, vol. 81, 115108 (2010).

[8] C. Lugini and M. Ronmano, "A ballistic-pendulum test stands to characterize small cold-gas thruster nozzle," *ACTA Astronautica*, vol. 64, issue5-6, 615-625, 2009.

[9] D. M. Gibbon, M. F. Paul, and T. Lawrence, "High-power, null-type, inverted pendulum thrust stand," *Proceedings of the 36th Joint Propulsion Conference and Exhibit*, Huntsville, AL, July 2000 unpublished.

[10] Q. E. Walker, W. Hargus, and M. A., "Cappelli, Characterization of a low-power helium arcjet," *Proceedings of the 34th Joint Propulsion Conference and Exhibit*, Cleveland, OH, July 1998 unpublished.

[11] D. H. Manzella, R. S. Jankovsky, and R. R. Hofer, "NASA's Hall thruster program 2002," Proceedings of the 38th Joint Propulsion Conference and Exhibit, Indianapolis, IN, July 2002 unpublished.

[12] Kunning G. Xu and Mitchell L. R. Walker, "High-power, null-type, inverted pendulum thrust stand," *Review of Scientific Instruments*, vol. 80, 055103, 2009.

[13] A.D. Ketsdever and E.P. Muntz, "Facility Effects on Performance Measurements of Micropropulsion Systems," *Proceedings of the 37th AIAA/ASME/ SAE/ASEE Joint Propulsion Conference*, Salt Lake City, UT, paper 2001-3335, 8–11 July 2001.

[14] A. D. Ketsdever, A. A. Green, and E. P. Muntz, "Momentum flux measurements from under expanded orifices: Applications for microspacecraft systems," AIAA paper 2001-0502, Proceedings of the 39th AIAA Aerospace Sciences Meeting, Reno, NV, 8–11 January 2001.

[15] W. D. Willis III, C. M. Zakrzwski, and S. M. Merkowitz, "Development of a Thrust Stand to meet LISA Mission Requirements," *Proceedings of the 38thAIAA/ASME/SAE/ ASEE Joint Propulsion Conferenc*e, Indianapolis, IN, 7–10 July 2002.

[16] H. Koizumi, K. Komurasaki, Y. Arakawa, "Development of thrust stand for low impulse measurement from microthrusters," *Review of Scientific Instrument*, vol. 75, no. 10, p. 3185, 2004.

[17] T. Stevenson and G. Lightsey, "Design and operation of a thrust test stand for university small satellite thrusters," *American Institute of Aeronautics and Astronautics*, 2018.

[18] J. Anderson, *Modern Compressible Flow with Historical Perspective*, 3rd ed. New York: McGraw-Hill, 2003.

[19] G.P. Sutton, O. Biblarz, *Rocket Propulsion Elements*, Wiley IEEE, New York, Chapter 3, 2001.

[20] H. Moazam Sheikh and et al, "Design of test bench for measurement of thrust and impulse bits of mems-based micro-thrusters", J*ournal of young investigators*, vol. 35, July 2018.

[21] C. Lugini and M. Romano, "A ballistic-pendulum test stand to characterize small cold-gas thruster nozzles," *Acta Astronautica,* vol. 64, 2009, pp. 615 – 625.